Chapter 3

Processing and nanoclay induced piezoelectricity in poly(vinylidenefluoride-co-hexafluoro propylene) nanohybrid

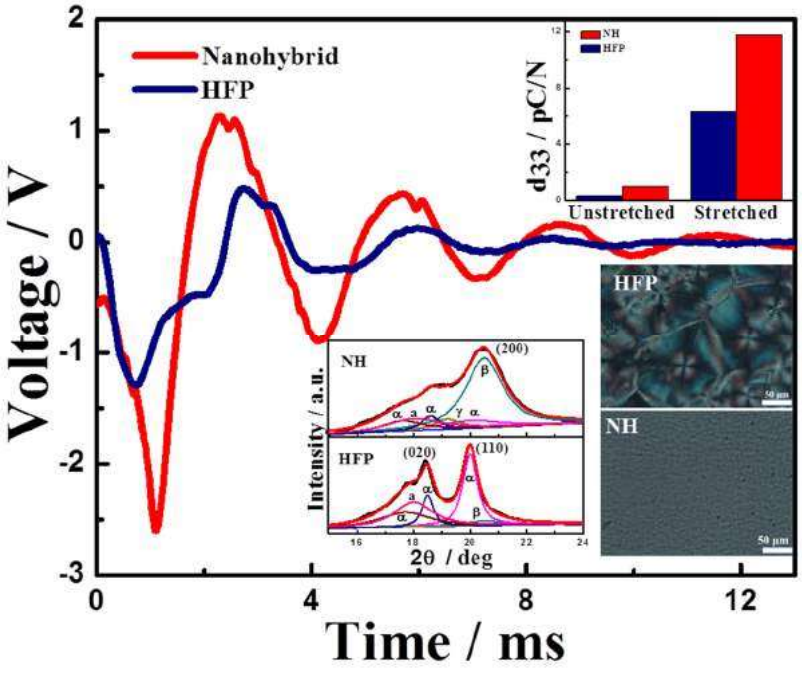

3.1. Introduction:

Fluoropolymers like poly(vinylidene fluoride) (PVDF) and its copolymers with hexafluoropropylene (P(VDF-co-HFP)) are of technological importance because of their capability to crystallize in different forms, especially few of them are piezoelectric in nature. These polymers have applications in several fields such as sensors and actuators [130, 131]. The crystalline structure of P(VDF-co-HFP) copolymer is similar to that of PVDF [132, 133] while its flexibility and chemical resistance are considerably higher [134, 134] due to lesser degree of crystallinity.

Two-dimensional nanoclay has greater advantage for structural amendment in presence of layered heterogeneity over the zero-dimensional fillers like silica and titania [135] where no change of structure is observed, or one-dimensional filler like CNT/nanorod [136], where there is a meager amount of β-phase on template due to dimensional constraints. It is apparent that the requirements of better compatibility and interaction of the filler and the matrix polymer is essential to generate the electroactive form in a polymer. Nanoclays are layered silicate in which tetrahedral and octahedral layers are fused together by sharing oxygen atoms. The structure of layered silicate is shown in **Figure 3.1**. Generally the layer thickness is ~1 nm and lateral dimension is ~30 nm to several microns. There are metal ions within the interlayer spacing, which can be replaced by alkylammonium or phosphonium by ion exchange, which increases the interplanar distance of clay. This makes clay hydrophobic and compatible to polymer. The advantage of using clay is that it has large surface area to interact with the polymer and also, the alkyl ammonium and alkylphosphonium ions can provide the functional groups [137].

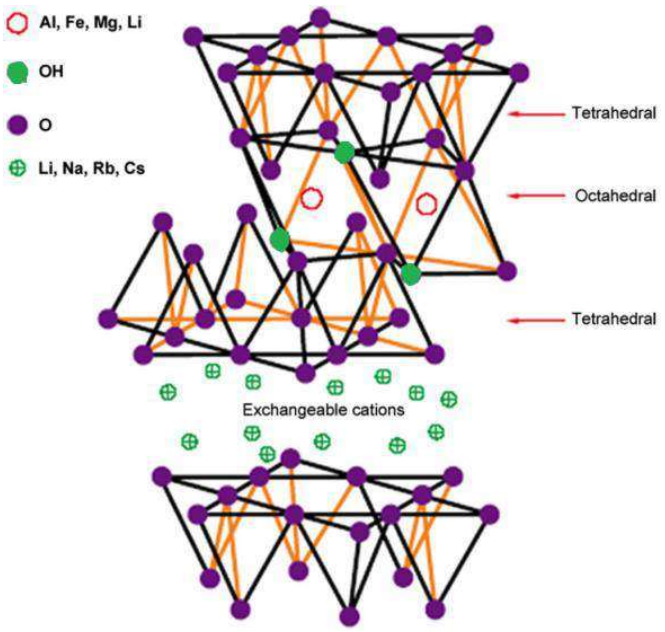

Figure 3.1: Structure of layered silicate [138].

Polar β-phase is the main factor for controlling the electronic properties and piezoelectric coefficient, d_{33} is a measure of the device performance. Stretching of the film is considered as one of the suitable methods to induce β-phase in polymer matrix, but the extent of the electronic phase restricts because of the brittleness of pure PVDF. Improvement in toughness in hybrid in presence of filler may help more piezoelectric β-phase to induce in fluoropolymers. Piezoelectric coefficient of PVDF in presence of nanoclay is also reported, where attempt of alteration of electronic structure is done by stretching at fixed draw ratio [90]. There is no report of the effect on piezoelectric coefficient of HFP copolymer in presence of nanoclay under uniaxial stretching at different temperatures and device performances thereof.

In the present work, nanoparticles and process induced super toughening phenomena has been revealed. The nanohybrids of poly(vinylidene fluoride-co-hexafluoro propylene) with

layered silicate is prepared through solution route. The morphology, nanostructures, crystalline structure, thermal and mechanical properties of the nanohybrids have been demonstrated in comparison to pure polymer. The extent of piezoelectric β-phase of nanohybrid has been enhanced to a significant amount under uniaxial elongation at different temperatures. The piezoelectric coefficient after the electric poling has been measured. A device has been fabricated using the developed nanohybrid and its performance was evaluated and compared with pure polymer under similar processing condition.

3.2. Experimental

Materials: Poly(vinyl fluoride-co-hexafluoropropylene) P(VDF-HFP). Organically modified clay, Cloisite 30B.

Preparation of nanohybrid: Hybrid of HFP and 30B clay has been prepared by solution method as discussed in **Chapter 2**.

HFP and hybrids are abbreviated as HFP and NH. The samples after stretching are denoted by HFP-S and NH-S.

3.3. Results and discussion:

3.3.1. Influence of nanoparticle on structure and nanostructure:

Nanoclay embedded in polymer matrix has strong influence on the structure of polymer attached and nanostructure of the nanoparticle. The clay platelets are well dispersed in HFP matrix showing discrete layers of nanoclay as well as some tactoids as observed through bright field TEM image (**Figure 3.2a**). The inter layer spacing of the pristine nanoclay (d001) disappears in nanohybrid presumably due to disordered structure cause by the insertion of

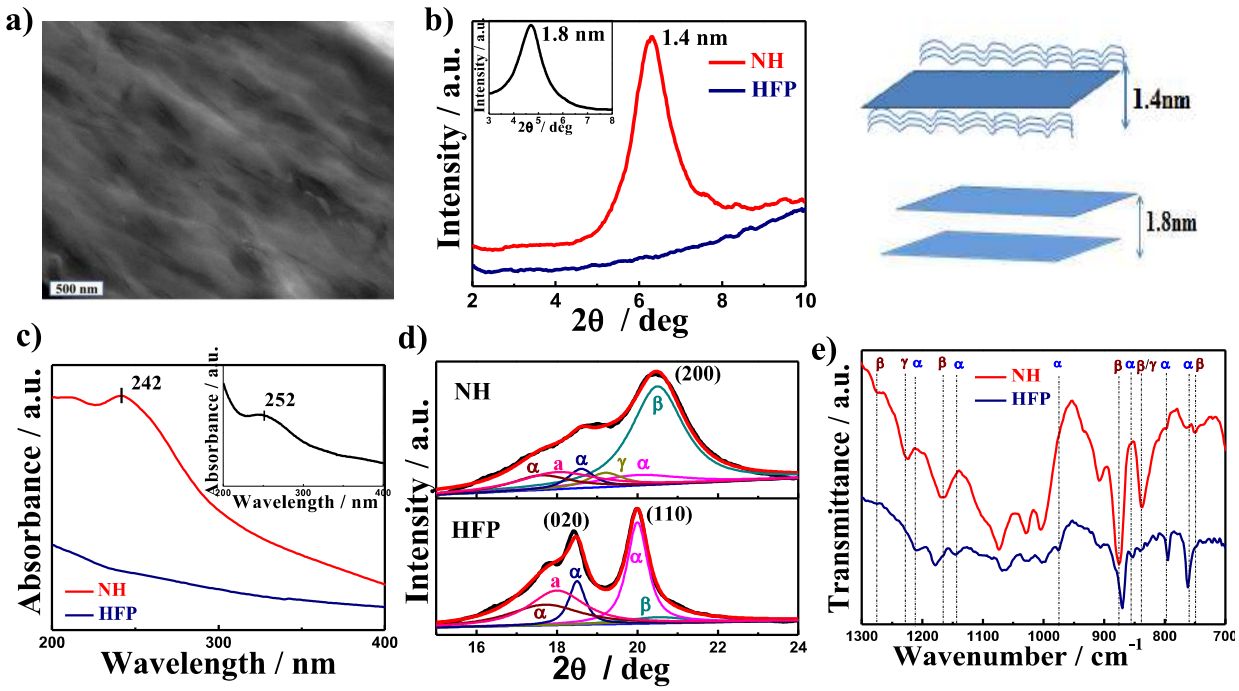

Figure 3.2: Structure and nanostructure a) Bright field transmission electron micrograph of HFP nanohybrid, b) nanostructure of hybrid and changes in interlayer spacing of clay after polymer insertion c) UV-vis absorption spectra of HFP and nanohybrid. Inset figure shows the absorption spectra of pristine organically modified nanoclay, d) XRD deconvoluted diffractograms of HFP and nanohybrid, showing different phases, and, e) FTIR spectra of pure HFP and nanohybrid indicating different peaks positions for α-, β- and γ-phases.

the long chain molecule within the gallery (**Figure 3.2b**). The intercalation of polymer molecules is primarily due to good interaction between nanoclay and HFP molecules as evident from the shifting of absorption peak at 252 nm of pristine nanoclay to 242 nm observed in nanohybrid (**Figure 3.2c**). The blue shift observed in nanohybrid arises from the constraint conformation caused by the insertion of polymer molecule inside the galleries. This is to mention that absorption peak of pristine nanoclay appears from the olefinic double bond present in the organic modifier of the nanoclay while pure HFP does not show any absorption band in the energy range studied.

Apart from good dispersion, nanoclay induces piezoelectric smaller crystallite of β-phase as observed through deconvoluted XRD peaks (**Figure 3.2d**) **[139]**. HFP crystallizes in β form in presence of nanoclay as clear from the peak at 2θ~20.6^o (200/110 planes) against only α-form of pure HFP. Shifting of deconvoluted peaks towards higher 2θ at 18.08^o (110), 18.6^o (020) and 20.0^o (110) peak in nanohybrid in comparison to 17.9^o (100), 18.5^o (020) and 19.9^o (110) peak position of α-phase in pure HFP and the appearance of a new peak at 2θ~19.0 in nanohybrid clearly indicates the formation of a metastable phase (distorted β or γ-conformation) in presence of nanoclay [140]. The crystallization of β-phase occurs on top and bottom of the silicate layers of nanoclay arising from the good interaction as mentioned earlier as revealed from the XRD peak position at 2θ~6.3^o corresponding to the interplanar distance of two crystallized zone below and above the individual silicate layer (**Figure 3.2b**) [141]. The amount of β-phase content is estimated to be 18% in nanohybrid against the meager 0.1% in pure HFP, as calculated from the deconvoluted area fraction (**Figure 3.2d**). However, considerable amount of α- and amorphous phases are present in nanohybrid as evident from the deconvoluted XRD peaks. Pure HFP shows FTIR absorption bands of α-phase at 760, 797, 857, 975, 1144 and 1210 cm^{-1} which disappear in nanohybrid and instead the peaks at 749, 840, 878, 1165 and 1276 cm^{-1} appear, assigned for either β- or γ-phase including their distorted conformations (**Figure 3.2e**) [142, 143]. Among these peaks, 840 cm^{-1} peak is due to both β- and γ-phase while the peak at 1227 cm^{-1} confirms the presence of γ phase in nanohybrid. However, the appearances of FTIR absorption bands at 749, 878, 1165 and 1276 cm^{-1} corresponds to pure β-phase occur in nanohybrid vis-a-vis pure HFP.

3.3.2. Processing induced phenomena:

Nanoclay induces the piezoelectric β-phase in HFP matrix but the extent is not sufficient (18%) for device application. Uniaxial stretching has been performed to induce more β-phase in presence of nanoparticle. To study the effect of stretching, pure HFP and nanohybrids samples are stretched at different temperatures (**Figure 3.3a**). As we can see that at room temperature there is no significant changes in the toughness and modulus, so we performed the stretching at elevated temperatures and found that the 90°C is the optimum temperature for stretching.

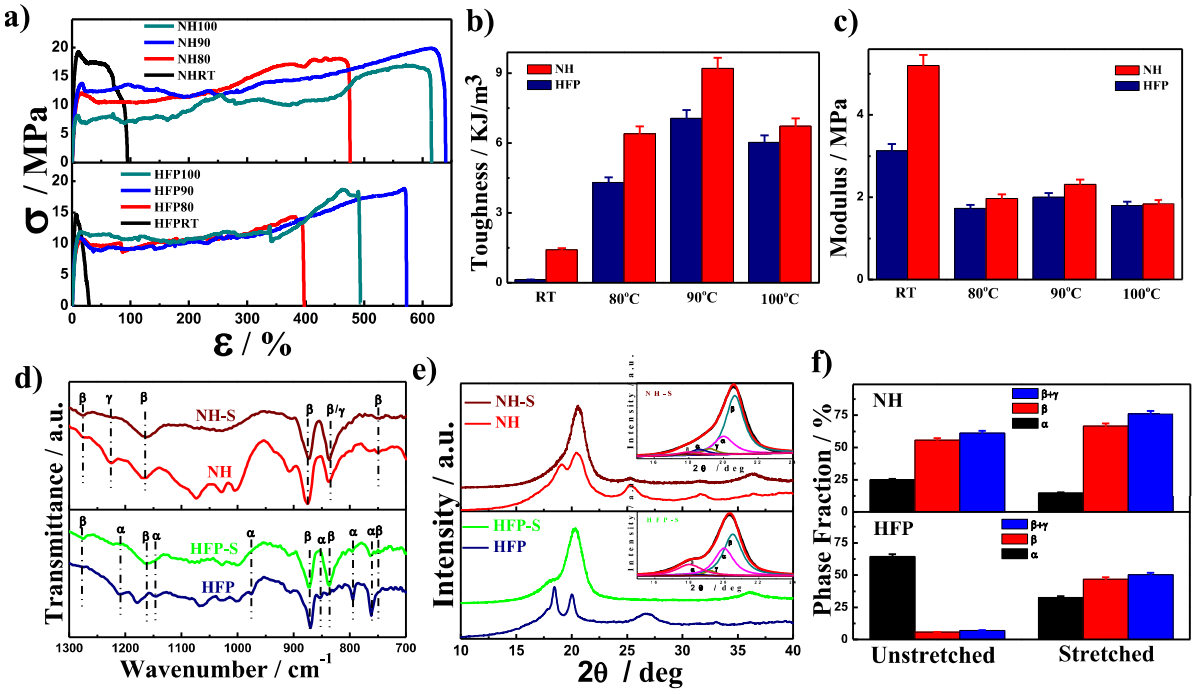

Figure 3.3: Effect of stretching a) Stress-Strain curve for Pure HFP and nanohybrid samples stretched at different temperature, corresponding (b) toughness and (c) modulus d) FTIR spectra of pure HFP and nanohybrid stretched samples, e) wide angle X-ray diffraction pattern of pure HFP and nanohybrid stretched samples at 90°C. Inset figures show the deconvoluted diffractograms of stretched specimen, and, f) Phase fraction of unstretched and stretched samples showing percentage of α-, β- and γ-phases.

At 90^{o}C the toughness, area under the curve is highest (**Figure 3.3b**) i.e. sample is more stretched at this temperature, which is a favorable condition for the piezoelectric phase generation. The modulus is highest at room temperature but almost constant with the temperature (**Figure 3.3c**). At the optimum stretching temperature, the toughness increases from 7 to 9.2 kJ/m^3 in nanohybrid as compared to pure HFP along with a considerable increase in stiffness in nanohybrid (1.06-1.59 MPa). This is worthy to mention that toughness values of pure HFP and its nanohybrid at room temperature are 0.2 and 0.7 kJ/m^3, respectively, much less (more than one order in magnitude) than the values measured at 90 ^{o}C. The significantly higher values of toughness in nanohybrid at the higher temperature (90 ^{o}C) arise from the greater elongation at break (95-640%) at higher temperature predominantly due to ease of deformation at lower viscosity. However, the extension has very much increased (~6 folds) under uniaxial elongation at a high temperature which helps to improve the alignment of polymer chains in the direction of force field. Hence, it is expected that β-phase content should increase after uniaxial stretching at a high temperature. **Figure 3.3d** compares the FTIR spectra of stretched samples vis-a-vis unstretched pure HFP and nanohybrid showing occurrences of distinct β-phase peaks at 749, 840, 880, 1168 and 1275 cm^{-1} in stretched samples against α-phase peaks at 759, 797, 854, 975, 1143 and 1211 cm^{-1} of unstretched HFP. This is to mention that the β-phase was present in unstretched nanohybrid while their intensities increase significantly after elongation and subsequently the peaks corresponding to the α-phase either disappear or diminished considerably.

Structural change over after stretching at high temperature is also endorsed through XRD measurements. A change of structure from α to β is evident from the appearance of a peak at 20.6^{o} due to (200/110) plane against 17.6^{o} (110), 18.6^{o} (020) and 20^{o} (110) of α-phase before

stretching of pure HFP (**Figure 3.3e**). Intensity corresponding to β-peak in nanohybrid has significantly been enhanced after stretching with the suppression of α-phase peaks. Further, XRD peak at 36.5^{o} also indicates the formation of β-phase after stretching both for HFP and its nanohybrid. The peaks are deconvoluted (inset of **Figure 3.3e**) and the β-phase fractions have been calculated from the ratio of the peak areas. It is clear that major α-phase in unstretched HFP has been converted into β- and γ-phase in nanohybrid while the extent of piezoelectric phase has significantly been increased after stretching (**Figure 3.3f**). The formation of γ-phase is considerably low as compared to β-phase after stretching both for HFP and NH. This is worthy to mention that both mechanical properties and electronic properties are their best at 90 ^{o}C stretched samples and the properties decrease both for increasing and decreasing the temperature of stretching. Hence, there is a direct correlation between the structural development and electronic properties, which is found to be optimized at 90 ^{o}C stretching condition.

Now, it is pertinent to correlate the structural development with uniaxial stretching. Higher elongation at break or greater draw ratio [90] increases the molecular chain alignment in the direction of force field and greater alignment helps the HFP chain to crystallize in micro fibrillar all-trans planar zigzag conformation of β-phase. The conversion of amorphous phase into β-phase due to stretching is evident from the fact that considerable reduction of amorphous phase content after elongation both in HFP and nanohybrid (35 to 20% in HFP against 25 to 12% in nanohybrid stretched at 90 ^{o}C) (**Figure 3.3f**). Amorphous to β-phase conversion due to stretching is apparent from the whitening of the film during elongation and increase of overall crystalline phase both for HFP and NH after stretching. Further, the formation of necking is considered as a starting point of the transformation from spherulitic

pattern to needle like morphology, responsible for β-phase conversion from the α-phase [144, 145]. However, higher β-phase is evident after stretching while the extent is significantly higher in nanohybrid and expects greater ferroelectric responses in nanohybrid in presence of nanoclay, nucleating agent of β-phase. Moreover, total 75% piezoelectric phase is observed in nanohybrid as opposed to only 50% noticed in pure HFP after controlled stretching at optimized conditions. Elongation temperature has a significant role towards β-phase transformation and much higher temperature (120 ^{o}C) increase the chain mobility causing crystallization of thermodynamically feasible α-phase [56, 144]. Thus, an optimized temperature window has been found to generate maximum transformation to β-phase for possible device applications.

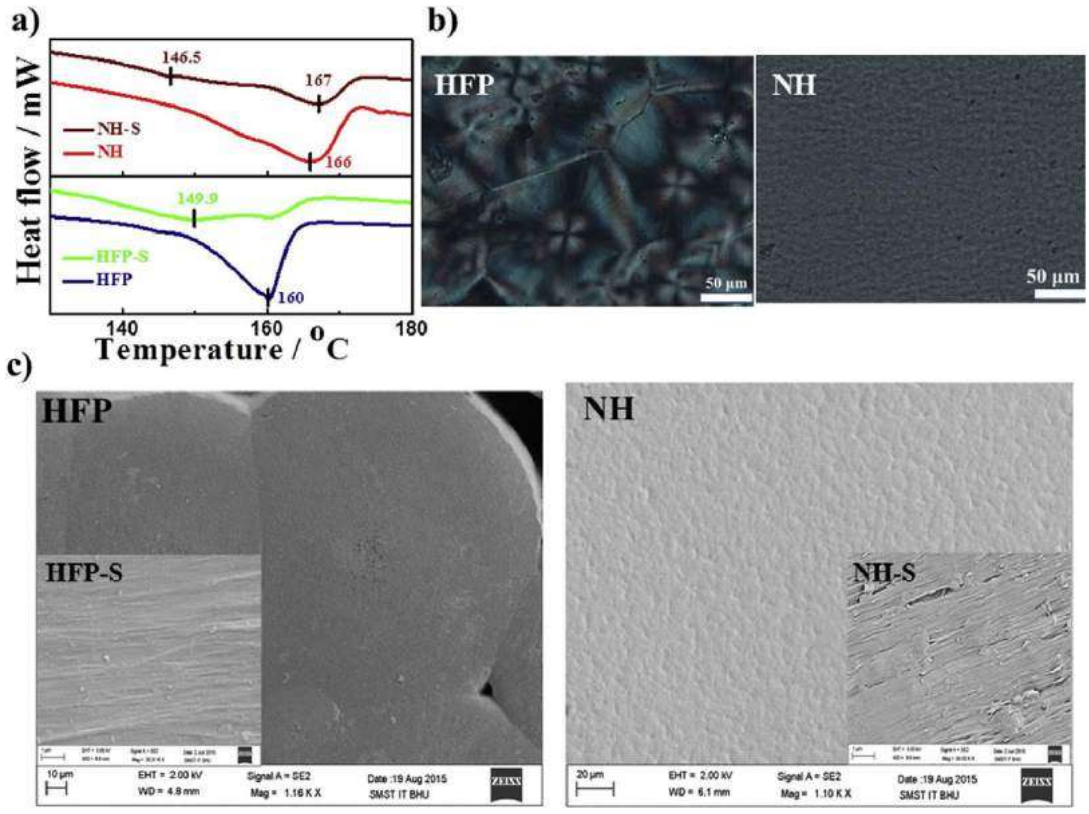

Figure 3.4: a) DSC thermograms of pure HFP and nanohybrid unstretched and stretched samples; HFP-S and NH-S represent specimens after stretching of respective sample, b) Polarizing optical microscope images of pure HFP and nanohybrid. No birefringence is observed in nanohybrid whereas spherulites were present in pure HFP, and, c) Scanning electron microscope image of pure HFP and nanohybrid. Inset figures show corresponding stretched sample images.

The evidence of formation of piezoelectric phases due to stretching is clear from the appearance of low melting peak at 149.9^{o}C in DSC thermograms after stretching of pure HFP in addition to the α-phase melting peak at 160 ^{o}C (**Figure 3.4a**). Higher melting peak of unstretched nanohybrid at 166 ^{o}C indicates the formation γ-phase in addition to the β-phase in presence of nanoclay as the order of melting temperature of the different phases is γ > α> β [90]. Interestingly, much lower melting at 146.5 ^{o}C in stretched nanohybrid is presumably due to more abundant β-phase as discussed earlier. Heat of fusion, calculated from the normalized area under the endothermic curve, decreases to 17.0 in nanohybrid in comparison to 25.2 J/gm in pure HFP as the heat of fusion of α and γ-phase is higher than that of β-phase [136]. Further reduction of heat of fusion is observed after stretching as 22.3 and 14.5 J/gm in HFP and nanohybrid, respectively, suggest the formation of more β-phase under uniaxial elongation. The crystalline phases are also manifested in the optical micrographs as evident from the well-defined spherulites in α-phase in HFP against the birefringence less morphology in nanohybrid due to tiny needle like crystallite of β-phase (**Figure 3.4b**) [146]. The lack of birefringence in nanohybrid is due to random orientation of smaller mesh-like β-crystallites [139] against the larger, highly ordered spherulitic structure observed in pure HFP. Higher magnification morphology as observed through SEM also supports the distinct spherulite in pure unstretched HFP vis-a-vis mesh-like morphology in nanohybrid (**Figure 3.4c**). Molecular reorganization due to stretching has a strong influence on oriented patterns

in the surface morphology of stretched samples (inset images of **Figure 3.4c**). However, the calorimetry and morphology support the formation of β-phase in presence of nanoclay whose extent enhances after stretching.

3.3.3. Piezoelectric responses and device fabrication

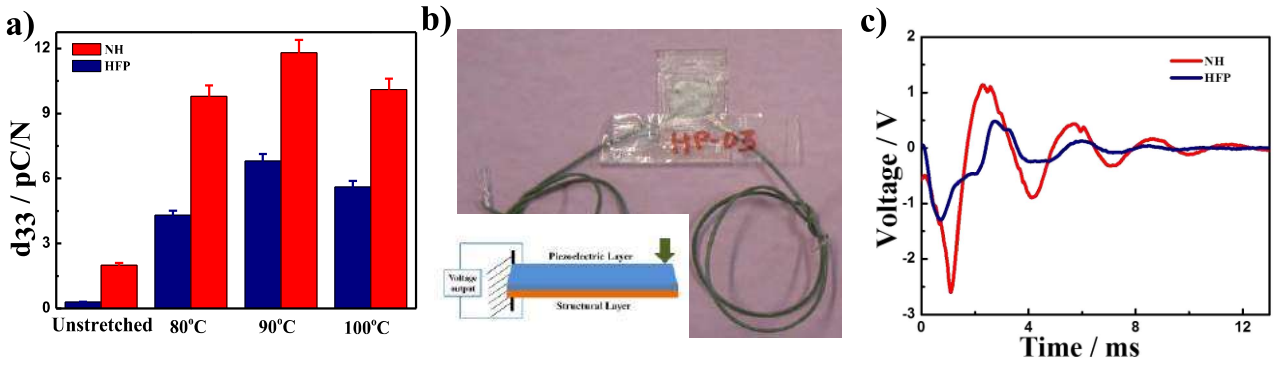

Figure 3.5: a) Bar diagram showing piezoelectric coefficient for pure HFP and nanohybrid before and after stretching at different temperatures b) Image of a fabricated unimorph, inset figure shows representation of assembly of device and, c) Output voltage response as a function of time.

Up to now, we have shown that the developed material is highly piezoelectric and pyroelectric especially in nanohybrid in presence of nanoclay and the piezoelectric phase has been increased considerably through processing of the nanohybrid. The piezoelectric coefficient, d_{33} is an important parameter for piezoelectric materials and values are reported in **Figure 3.5a**. The unstretched samples show very low d_{33} values of 0.3 and 1 pC/N for pure HFP and nanohybrid, respectively, while the corresponding values increase considerably to 6.8 and 12 pC/N after stretching at 90°C (poled at 450 kV/cm) indicating improvement in piezoelectricity due to induction of β-phase in presence of nanoclay and induced through uniaxial elongation. Further, much higher value of d_{33} (16 pC/N) is observed for HFP after stretching when it is poled at higher electric field (1000 kV/cm) However, it is

pertinent to mention that higher β-phase content samples, either in presence of nanoclay or induced through processing, show greater d_{33} values which are suitable for piezoelectric devices.

We have fabricated the unimorph using the high piezoelectric coefficient materials NH and HFP following the technique as mentioned in the experimental section. **Figure 3.5b** and inset figure shows the image of unimorph and representation of assembly of device. The voltage responses under impulse load are compared for HFP and nanohybrid as a function of time (**Figure 3.5c**). It is clear that nanohybrid shows the greater voltage generation along with longer time response vis-a-vis HFP. The unimorphs clearly demonstrate the superior piezoelectric device made using nanohybrid where the extent of piezoelectric phase is considerably higher. In brief, novel piezoelectric polymer nanohybrid has been developed using two dimensional nanoparticle and thereby applying special processing technique with greater coefficients which shows considerably greater piezoelectric device performance. Moreover, the novel piezoelectric properties of developed nanohybrid are of greater values for future applications.

3.4. Conclusions

The nanohybrid of HFP copolymer with organically modified nanoclay has been prepared through solution route. Finer dispersion of nanoclay in polymer matrix along with blue shift in UV absorption indicates the good interaction between the components. Nanoclay induces the piezoelectric β-phase in polymer which is further enhanced through processing technique by uniaxial stretching at moderately high temperature. Improvement in mechanical properties, both stiffness and toughness, of nanohybrid has been reported as compared to

pure HFP. The maximum value of all-trans planar zigzag conformation of β-phase (75%) was obtained at 90 ^{o}C under stretching. The structural change over and its quantitative measurement has been confirmed through XRD, FTIR, POM and DSC studies. The enhancement of piezoelectric β-phase in nanohybrid has been reflected in higher piezoelectric coefficient than that of pure HFP. The unimorphs are made using higher coefficient of HFP and its nanohybrid samples. The voltage response under impulse load is much higher in nanohybrid as compared pure HFP along with the longer response time indicating much better piezoelectric device performance using nanohybrid.